Available online at www.sciencedirect.com
ScienceDirect
Trans. Nonferrous Met. Soc. China 26(2016) 1170−1175
Transactions of Nonferrous Metals Society of China
www.tnmsc.cn

Bimodal-grained Ti fabricated by high-energy ball milling and spark plasma sintering

Yan LONG, Wen-jing GUO, Ying LI

Guangdong Provincial Key Laboratory of Metal Processing and Forming, School of Mechanical and Automotive Engineering, South China University of Technology, Guangzhou 510640, China

Received 2 April 2015; accepted 11 January 2016

Abstract: Bimodal-grained Ti containing coarse and fine grains was fabricated by high-energy ball milling and spark plasma sintering (SPS). The microstructure and mechanical properties of the compacts sintered by Ti powders ball-milled for different time were studied. Experimental results indicated that when the ball-milling time increased, the microstructure of sintered Ti was firstly changed from coarse-grained to bimodal-grained structure, subsequently transformed to a homogeneous fine-grained structure. Compared with coarse-grained Ti and fine-grained Ti, bimodal-grained Ti exhibited balanced strength and ductility. The sample sintered from Ti powders ball-milled for 10 h consisting of 65.3% (volume fraction) fine-grained region (average grain size 1 μm) and 34.7% coarse-grained region (grain size > 5 μm) exhibited a compress strength of 1028 MPa as well as a plastic strain to failure of 22%.

Key words: titanium alloy; high-energy ball milling; spark plasma sintering; bimodal-grained structure

1 Introduction

Pure titanium has low density, excellent corrosion resistance and biocompatibility. However, it exhibits lower strength, which limits its use for structural and functional applications. For many engineering and biomedical applications, high strength is required. Bulk metallic materials with fine grains were produced by severe plastic deformation, casting and powder metallurgy method [1−3]. The grain sizes were reduced into micron, sub-micron and nanometer scale, therefore the mechanical strengths of metals were much higher than that of their conventional coarse-grained counterparts [4−6]. Besides the grain size, the distribution of grain size may also play an important effect on the mechanical properties of metals and alloys. Recent researches revealed that compared with homogeneous nanostructured metals, bimodal or multimodal nanostructured metals could exhibit better combination of strength and ductility [7]. For example, WANG et al [8] reported nanocrystalline Cu with a multimodal grain size distribution processed by a thermomechanical treatment. The presence of micrometer-size grains in a matrix of nanocrystalline and ultrafine grains led to a high tensile elongation of 65% as well as maintaining a high strength 5−6 times higher than that of coarse-grained Cu. ERTORER et al [9,10] previously reported a bimodal ultrafine-grained commercially pure Ti fabricated by cryomilling and sintering. In those studies, a broad grain size distribution in Ti resulted in enhanced tensile strength in combination with high ductility.

One of the widely used methods to produce metallic materials with fine grains is high-energy ball milling. It was reported that this process easily formed nano-grains with a diameter of 20 nm for Ti and Ti−6Al−4V [11,12]. However, a wide distribution of grain size may exist in the ball milled powders before a homogeneous nanostructure was achieved. Therefore, bimodal or multimodal microstructure could be achieved by this traditional technique. The present study was to fabricate pure titanium bulky material with a bimodal-grained structure by high-energy ball milling and spark plasma sintering (SPS). Pure titanium powders were firstly ball-milled for different time and subsequently consolidated

Foundation item: Project (51104066) supported by the National Natural Science Foundation of China; Projects (2015A010105011, 2015A020214008) supported by Science and Technology Program of Guangdong Province, China; Project (201505040925029) supported by Science and Technology Research Program of Guangzhou, China

Corresponding author: Yan LONG; Tel: +86-13600465918; E-mail: ylong1@scut.edu.cn

DOI: 10.1016/S1003-6326(16)64216-4

by spark plasma sintering (SPS), which is a fast consolidation approach with the activation of a pulsed electrical field [13]. Compared with conventional sintering methods, SPS has shorter sintering time and lower sintering temperature, therefore, it is effective to restrain the grain growth during the sintering process [14−16]. The effects of ball milling time on the microstructure and compressive properties of sintered Ti were investigated and the microstructure evolution of ball-milled powders during sintering process was discussed in the present work.

2 Experimental

Commercially pure titanium powders with the purity of 99.7% were produced by plasma rotating electrode atomization process. The average particle size of original powders was 150 μm. The powders were milled in a QM−2SP20-CL planetary ball milling machine with stainless steel containers and balls and the ball to powder ratio was 12:1. The ball milling was performed at a speed of 228 r/min in an argon atmosphere for 5, 10, and 50 h, respectively.

The unmilled powders and as-milled powders with various milling time were sintered by SPS at 750 °C under a vacuum of $<10^{-3}$ Pa. A uniaxial pressure of 50 MPa was applied on the powders during the sintering process. The powders were heated to the maximum temperature at a heating rate of 100 °C/min, and held for 4 min. The load was removed when the furnace was cooled to lower than 200 °C.

The sintered samples with a thickness of 12 mm and diameter of 10 mm were ground and polished to remove surface contamination before conducting microstructure characterization. The microstructures of bulk specimens after sintering were observed by LEICA DMI 5000M optical metallographic microscope. The densities were measured by Archimedes method using water as a liquid medium. Vickers hardness was tested at a load of 4.9 N for 20 s by HVS−1000 hardness testing machine. The compressive test was performed at a strain rate of 1×10^{-3} s^{-1} on a MTS Test Star 810 testing machine at room temperature. Specimens used in compressive test were cylinders with a thickness of 6 mm and diameter of 3 mm.

3 Results and discussion

The densification curves obtained by recording the changes of punch displacements during the heating process up to 900 °C are shown in Fig. 1.

It can be seen from Fig. 1 that when the sintering temperature reaches 900 °C, the densification curve of unmilled powders is still ascending, which indicates that at the heating rate of 100 °C/min, the densification temperature of those powders is higher than 900 °C. However, the densification curves of powders ball-milled for 5, 10 and 50 h have arrived at steady plateaus at 750 °C and their densification processes are basically completed. Additionally, the densification temperature of ball-milled powders decreases with the increase of ball milling time. During the ball milling process, the microstructures of powders were refined gradually by severe plastic deformation. The ball-milled powders have higher dislocation densities and larger grain boundary surfaces than the unmilled powders, which led to the acceleration of atom diffusion and sintering process. Therefore, the densification curves for ball-milled Ti powders showed a much lower densification temperature than the unmilled powders.

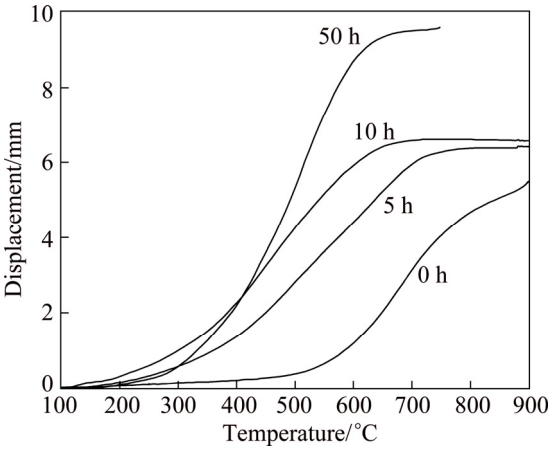

Fig. 1 Densification curves of Ti powders ball-milled for different time

The microstructures of the samples sintered with Ti powders ball-milled for different time are shown in Fig. 2. It is found that a large number of pores are distributed on particle boundaries in the sample sintered from unmilled powders. This indicates that the powders are not sintered sufficiently due to the relatively low sintering temperature (Fig. 2(a)). The microstructures of the sintered samples mainly consist of equiaxed grains with some acicular structures distributed in them. It is suggested that equiaxed grains are generated in most of the powders due to recrystallization, while in other powders, the original acicular structures in the atomized powders are still maintained.

In the sample sintered with powders ball-milled for 5 h, few pores could be seen and a netlike structure consisting of dark and bright regions is formed, as shown in Fig. 2(b). The dark regions distributed on the boundaries of original particles are found to be composed of finer grains with the average grain size of about 1 μm. The bright regions distributed in the interior of particles, however, consist of coarser grains with the

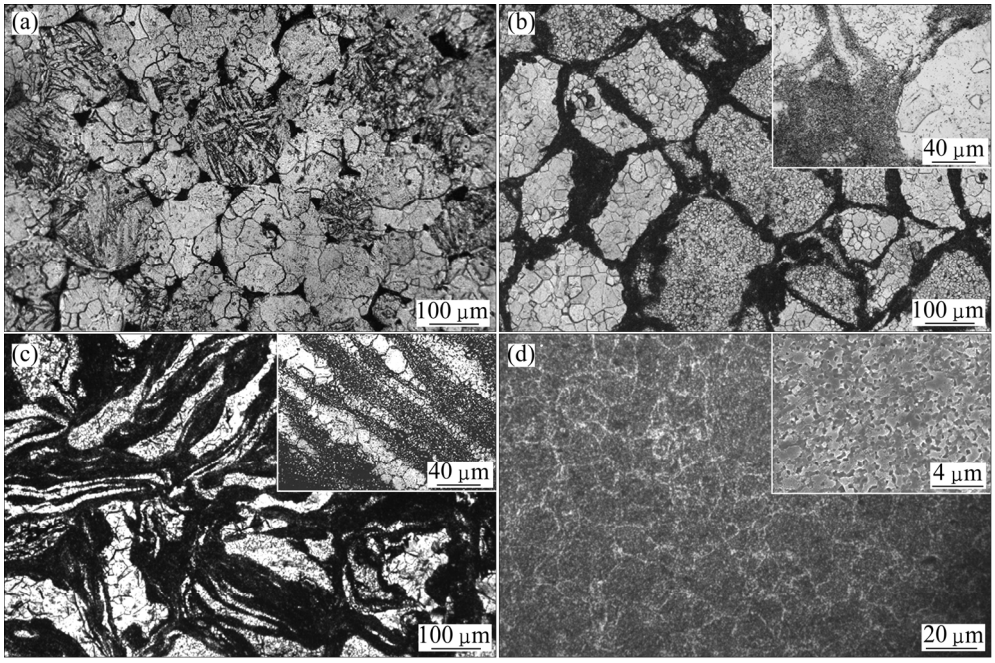

Fig. 2 Metallographic microstructures of samples sintered with Ti powders ball-milled for different time: (a) 0 h; (b) 5 h; (c) 10 h; (d) 50 h (the upright insets showed the magnification or SEM graphs of corresponding samples)

grain sizes larger than 5 μm. When the ball milling time increase to 10 h, the microstructure of sintered sample turns into a lamellar morphology with coarse-grained and fine-grained regions distributed alternately, which is due to the severe plastic deformation in ball milling process, as shown in Fig. 2(c). Compared with the sintered sample with the ball milling time of 5 h, the volume fraction of fine-grained regions in the 10 h-milled samples is apparently increased. As the milling time increase to 50 h, the microstructure in the sintered sample finally changes to homogenous fine-grained structure, and the average grain size is about 1 μm, as shown in Fig. 2(d). The densities and grain size distribution in sintered samples are shown in Table 1.

Table 1 Densities and grain size distribution in sintered samples with different ball milling time (FG: fine-grained region; CG: coarse-grained region)

Ball milling time/h	Relative density/%	Grain size/μm		Volume fraction/%	
		FG	CG	FG	CG
0	93.2	−	10−80	0	100
5	98.0	~1	5−50	29.5	70.5
10	97.9	~1	5−50	65.3	34.7
50	97.8	~1	−	100	0

The formation of bimodal-grained structure in the sintered samples with the milling time of 5−10 h could be attributed to inhomogeneity of plastic strains in the ball-milled powders. Taking the single powder into account, a powder ball-milled for relatively short time showed different microstructures in the interior and surface region, because the latter has experienced heavier plastic deformation and the dislocation density increases dramatically. During the ball milling process, the microstructure near the powder surface gradually turns into dislocation cells, subgrains and fine grains, finally creating a thin layer of fine-grained region near the powder surface. While in the center of ball-milled powder, the plastic strain is much lower so that the grains are much coarser. Figures 3(a) and (b) demonstrate the TEM graphs of Ti powders ball-milled for 10 h. It is found that in Fig. 3(a), the average grain size of ball milled powders is decreased to about 50 nm, while Fig. 3(b) shows a coarser grain with the size of about 200 nm. This indicates that the grain sizes in ball milled powders are distributed in a wide range of several tens to hundreds of nanometer. After the sintering process, the microstructure inhomogeneity originated in ball-milled powders is still maintained even some grain growth occurred. Figures 3(c) and (d) show the fine-grained and coarse-grained regions in the sintered sample, respectively. It could be found that the fine-grained regions consist of equiaxed grains with the average grain size of 1 μm. Few dislocations could be seen inside these grains. The grain sizes in coarse-grained regions vary from 5 to 50 μm. Additionally, in some of the coarse-grained regions, high density of dislocations generated in the ball milling process still remained. When the ball milling time increases, the plastic deformation is enhanced, the fine-grained layer grows thicker and thicker, therefore leading to an increasing volume

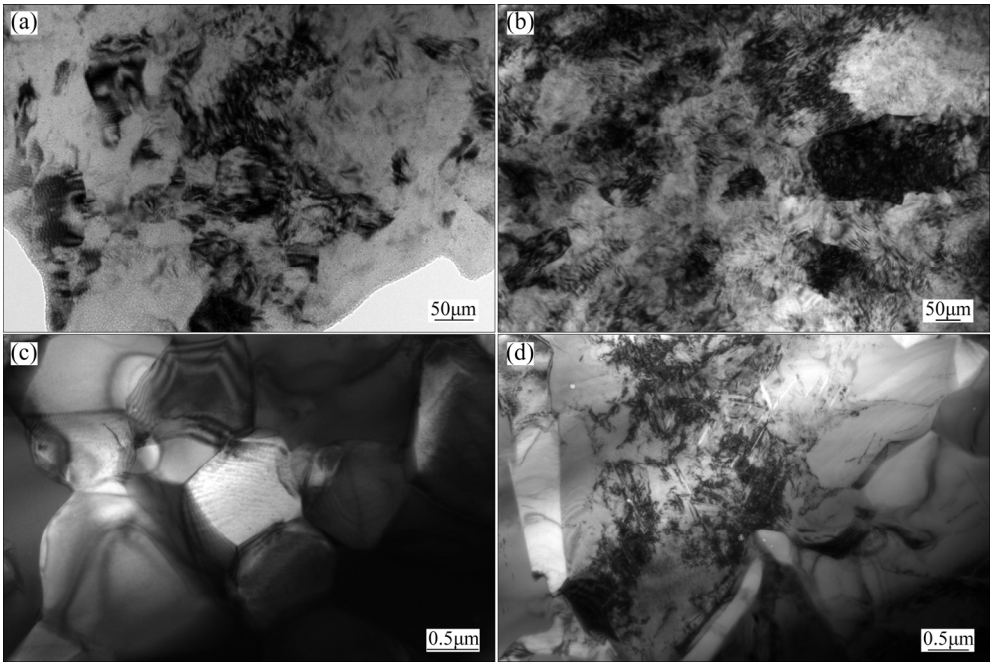

Fig. 3 TEM images of Ti ball-milled powders and sintered sample: (a) FG region in ball milled powders; (b) CG region in ball-milled powders; (c) FG region in sintered samples; (d) CG region in sintered samples (ball milling time 10 h, sintering temperature 750 °C, sintering time 4 min)

fraction of fine-grained regions in sintered sample until a homogeneous microstructure is finally obtained.

Figure 4 shows the Vickers hardness of the sintered samples with different ball-milling time. It should be noted that microhardness increases with increasing milling time. Moreover, in the bimodal-structured samples sintered from 5 h-milled and 10 h-milled powders, the hardness in fine-grained (FG) regions is significantly higher than that of coarsed-grain (CG) regions. The improvement of hardness in FG regions is not only caused by the grain refinement strengthening effect, but also related to the increasing content of impurities such as O, N, and Fe in these regions due to the increasing milling time.

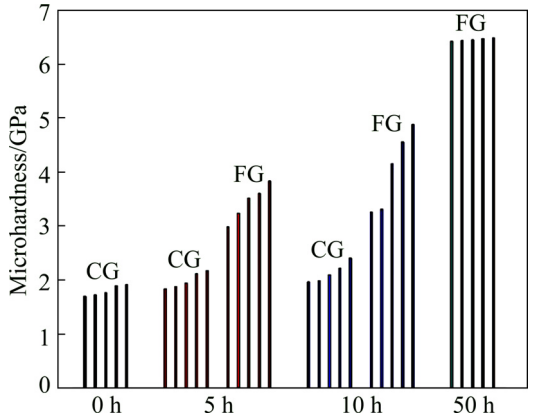

Fig. 4 Vickers hardness of samples sintered with Ti powders ball-milled for different time

Figure 5 shows the compressive engineering stress−strain curves of the sintered samples with various ball-milling time. The value of yield strength σ_{cy} increases with the increasing milling time, meanwhile, the plastic strain to failure ε_p decreases obviously. It is reported that in the bimodal microstructures, fine-grained regions act as strengthening phase according to Hall−Petch relationship while coarse grains enhance the ductility of the materials as toughening phases due to their good dislocation storage capability [8]. Therefore, it is reasonable that when the volume fraction of fine-grained regions increases with the ball milling time,

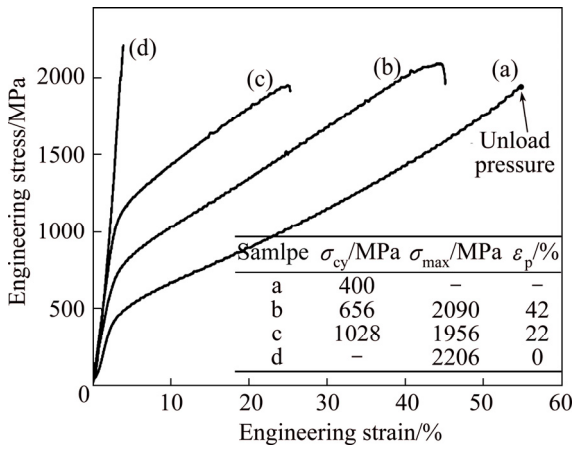

Fig. 5 Compressive stress−strain curves of samples sintered with Ti powders ball-milled for different time: (a) 0 h; (b) 5 h; (c) 10 h; (d) 50 h (sintering temperature 750 °C, sintering time 4 min)

the strength of sintered Ti is improved and the ductility is reduced. Compared with the sample sintered from unmilled powders, σ_{cy} values of the samples sintered by 5 h-milled and 10 h-milled powders are 64% and 157% higher, respectively. Additionally, those specimens show steady strain hardening stages after the yielding point, indicating that they maintain enough ductility as well. When the ball-milling time increases to 50 h, the ductility of the sintered sample is decreased to almost zero although the fracture strength was developed to about 2.2 GPa. Obviously, impurity elements introduced by ball milling process improve the compressive strength, but reduce the ductility markedly on the other hand.

Figure 6 shows the fracture morphologies of the samples sintered from 10 h-milled and 50 h-milled powders. As the 10 h-milled sample shows a bimodal microstructure, the fracture surface exhibits a mixed morphology with the smooth fracture surfaces and shear dimples dispersed alternately, as shown in Figs. 6(a) and (b). Although the fine-grained regions possess a higher value of yield stress, dislocation slipping is somewhat restrained by the grain boundaries, resulting in a reduced plasticity and showed smooth and smeared fracture morphology. However, the coarse-grained regions exhibit better plasticity because large-scale dislocation slipping is enabled. During the fracture process, crack propagates quickly in fine-grained regions. When the crack tips reach the coarse grained regions, they are blunted and deflected, consequently the crack propagation is impeded. Coarse-grained regions finally exhibit ductile fracture morphology consisting of shear dimples with the average size of 5−10 μm. In the case of the fine-grained Ti sintered from 50 h-milled powders, the fracture surface is characterized by river pattern in Figs. 6(c) and (d) and intergranular and transgranular fracture feature could be observed. Because of the limited ability of plastic deformation, cracks quickly propagate in the fracture process and finally exhibit cleavage fracture pattern. Therefore, in the sintered Ti fabricated by high energy ball milling and spark plasma sintering, the milling time should be controlled to obtain a balanced strength and ductility.

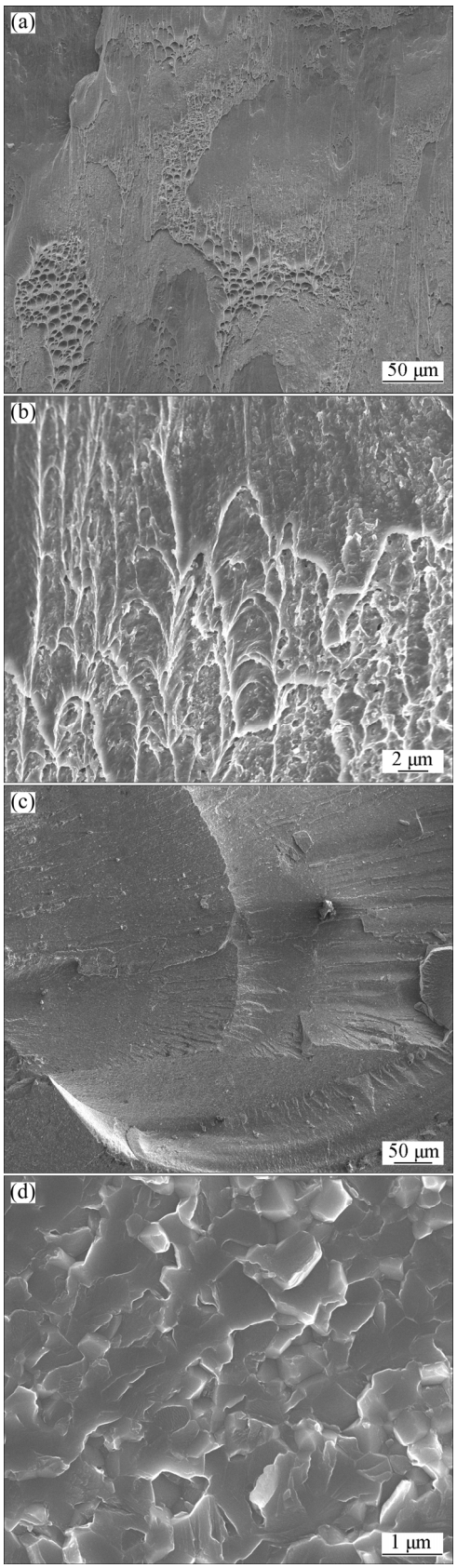

Fig. 6 Fracture morphologies of samples sintered with ball-milled Ti powders: (a, b) Ball-milling time 10 h; (c, d) Ball-milling time 50 h (sintering temperature 750 °C, sintering time 4 min)

4 Conclusions

1) When the ball-milling time increased from 0 to 50 h, the sintering temperature of titanium powders was dramatically decreased. The densities of samples sintered from ball-milled powders were developed compared to the unmilled samples.

2) When the milling time increased, the sintered samples changed from a coarse-grained to bimodal-grained structure, the volume fraction of fine-grained regions increased gradually, until finally a homogeneous fine-grained microstructure was obtained.

3) The hardness, compressive yield strength and fracture strength of the sintered sample increased obviously, while the plastic strain to failure decreased gradually with the increase of ball milling time. The bimodal-grained samples exhibited mixed fracture morphologies with the smooth fracture surfaces and shear dimples dispersed alternately. The fine-grained Ti sintered from 50 h-milled powders, however, showed a cleavage fracture pattern.

References

[1] VALIEV R Z, ISLAMGALIEV R K, ALEXANDROV I V. Bulk nanostructured materials from severe plastic deformation [J]. Progress in Materials Science, 2000, 45: 103−189.

[2] HE G, ECKERT J, L□SER W, SHULTZ L. Novel Ti-base nanostructure-dendrite composite with enhanced plasticity [J]. Nature Materials, 2003, 2(1): 33−37.

[3] ERTORER O, ZÚÑIGA A, TOPPING T, MOSS W, LAVERNIA E J. Mechanical behavior of cryomilled CP-Ti consolidated via quasi-isostatic forging [J]. Metallurgical and Materials Transactions A, 2009, 40(1): 91−103.

[4] MEYERS M A, MISHRA A, BENSON D J. Mechanical properties of nanocrystalline materials [J]. Progress in Materials Science, 2006, 51: 427−556.

[5] KUMAR K S, SWYGENHOVEN H V, SURESH S. Mechanical behavior of nanocrystalline metals and alloys [J]. Acta Materialia, 2003, 51: 5743−5774.

[6] SERGUEEVA A V, STOLYAROV V V, VALIEV R Z, MUKHERJEE A K. Advanced mechanical properties of pure titanium with ultrafine grained structure [J]. Scripta Materialia, 2001, 45(7): 747−752.

[7] MA E. Instabilities and ductility of nanocrystalline and ultrafine grained metals [J]. Scripta Materialia, 2003, 49(7): 663−668.

[8] WANG Yin-min, CHEN Ming-wei, ZHOU Feng-hua, MA En. High tensile ductility in a nanostructured metal [J]. Nature, 2002, 419(6910): 912−915.

[9] ERTORER O, TOPPING T D, LI Y, MOSS W, LAVEMIA E J. Nanostructured Ti consolidated via spark plasma sintering [J]. Metallurgical and Materials Transactions A, 2011, 42: 4964−4973.

[10] ERTORER O, TOPPING T D, LI Y, MOSS W, LAVERNIA E J. Enhanced tensile strength and high ductility in cryomilled commercially pure titanium [J]. Scripta Materialia, 2009, 60: 586−589.

[11] SUN F, ROJAS P, ZÚÑIGA A, LAVERNIA E J. Nanostructure in a Ti alloy processed using a cryomilling technique [J]. Materials Science and Engineering A, 2006, 430(1): 90−97.

[12] SOUFIANI A M, KARIMZADEH F, ENAYATI M H. Formation mechanism and characterization of nanostructured Ti6Al4V alloy prepared by mechanical alloying [J]. Materials & Design, 2012, 37: 152−160.

[13] OMORI M. Sintering, consolidation, reaction and crystal growth by the spark plasma sintering [J]. Materials Science and Engineering A, 2000, 287: 183−188.

[14] KUBOTA M, WYNNE B P. Electron backscattering diffraction analysis of mechanically milled and spark plasma sintered pure aluminium [J]. Scripta Materialia, 2007, 57: 719−722.

[15] DUAN R G, ZHAN G D, KUNTZ J D, KEAR B H, MUKHERJEE A K. Spark plasma sintering (SPS) consolidated ceramic composites from plasma-sprayed metastable Al_2TiO_5 powder and nano-Al_2O_3, TiO_2, and MgO powders [J]. Materials Science and Engineering A, 2004, 373: 180−186.

[16] CHA S I, HONG S H, KIM B K. Spark plasma sintering behavior of nanocrystalline WC−10Co cemented carbide powders [J]. Materials Science and Engineering A, 2003, 351: 31−38.

高能球磨–放电等离子烧结制备双尺度细晶钛

龙 雁，郭文晶，李 颖

华南理工大学 机械与汽车工程学院 广东省金属新材料制备与成形重点实验室，广州 510640

摘 要：采用高能球磨和放电等离子烧结技术制备出包含粗晶区和细晶区的双尺度细晶钛，并研究不同球磨时间的钛粉烧结试样的显微组织和力学性能。实验结果表明，随着球磨时间的增加，钛粉烧结试样的显微组织先由粗晶转变为双尺度晶粒，随后又转变为均匀的细晶组织。与单一尺度的粗晶钛和细晶钛相比，双尺度细晶钛具有更好的强度和塑性的组合。在球磨 10 h 钛粉烧结后的试样中，细晶区(平均晶粒尺寸为 1 μm)和粗晶区(晶粒尺寸大于 5 μm)的体积分数分别为 65.3%和 34.7%，其压缩强度达到 1028 MPa，同时断裂时的塑形应变达到 22%。

关键词：钛合金；高能球磨；放电等离子烧结；双尺度结构

(Edited by Yun-bin HE)